

RESEARCH ARTICLE

Analysis of Grain Morphology, Mineral Composition, and Ore Grade on Gold Placer Deposits in Bantimurung, Pangkep Regency, South Sulawesi, Indonesia

Angga Al Amin Husain¹, Ulva Ria Irfan^{1*}, Irzal Nur²

¹ Geological Engineering Department, Faculty of Engineering, Hasanuddin University, Makassar, Indonesia.

² Mining Engineering Department, Faculty of Engineering, Hasanuddin University, Makassar, Indonesia.

* Corresponding author : ulvairfan@yahoo.com

Tel.: +62-811466670; fax: +62-411840216

Received: Mar 21, 2022; Accepted: Jun 30, 2022.

DOI: 10.25299/jgeet.2022.7.2.9164

Abstract

The information through social media shows that there is quite an intense placer mining activity by local residents in the Bantimurung area, Tondong Tallasa District, Pangkep Regency. This study as a preliminary research aims to determine the grain morphology characteristics of mineral composition and metal grade in gold placer deposits in the study area. The data collected were eight samples. The collected samples were prepared into thin section, polished and observed using a microscope to identify the mineral composition and grain morphology. The grades of Au metal and its associated metals consisting of Ag, Zn, Pb, and Cu in the placer samples were analyzed by the AAS method. Petrography shows abundant of quartz, plagioclase, biotite and pyroxene minerals it might be indication of mineralization of epithermal. Ore petrography shows pyrite present along the river, silver is also found quite a lot along the river. Meanwhile, covellite, magnetite, sphalerite, and garnet were found only slightly at the sampling station this mineral composition indicates that the source of the placer deposits was epithermal. The grain morphology of the thin-section observation shows that quartz dominant has a high sphericity with character of roundness tends to be very angular to sub-rounded from upstream to downstream of the river. Plagioclase tends to have sub rounded roundness and high sphericity. Biotite tends to have a high sphericity with roundness from upstream to downstream is very angular, then angular, then sub-rounded. Pyroxenes tend to have high sphericity with very angular and angular roundness. Au content is directly proportional to Cu and inversely proportional to Zn, Pb, and Ag. Statistically Au affects the content of Cu by 50.97%. It can be concluded that Au is genetically associated with Cu, however Au grains that were still attached to the mineral and had not been separated from other minerals so that it could not be seen visually. This can also indicate that the source of this placer deposit is not far from the study site. Au grade correlated with stream sediment types it is 97,86 ppm for channel bar and 94,16 ppm for point bar, based on this we conclude the downstream has higher grade of Au compare to the upstream.

Keywords: Grain Morphology, Placer Deposits, Stream Sediment, Baturappe-Cindako Volcanic, Bantimurung,

1. Introduction

Information through social media shows that there is quite an intense placer mining activity by local residents in the Bantimurung area, Tondong Tallasa District, Pangkep Regency. Based on the results of field observation, information was obtained that this mining activity has been going on for decades, with productivity reaching 10 gram per day, with a large number of mining scattered along the river (Fig 1).



Fig. 1. Activities of residents panning for gold in the study area

South Sulawesi Province in regional geology is located in the Magmatic-Plutonic-Volcanic Tertiary Arc of West Sulawesi (Darman and Sidi, 2000; Hall and Wilson, 2000).

In this region, mineralization and hydrothermal gold deposits are only dominantly found in the North Sulawesi region, which is an active magmatic arc area (Carlile et al., 1990; Carlile and Mitchell, 1994; Kavalieris et al., 1992). There are very few indications and the presence of hydrothermal gold deposits in South Sulawesi Province which is a shoshonitic K-alkaline arc. The gold mineralization prospects that have been reported in the South Sulawesi region are only in the Sasak district, Tana Toraja (Cu-Au porphyry); Awak Mas, Luwu (mesothermal Au); and Palopo (anomaly Au-Pb-Zn-Cu and quartz-carbonate veins containing gold) (Idrus et al., 2017; Idrus and Nur, 2011; Nur et al., 2015; van Leeuwen, 2018; van Leeuwen and Pieters, 2011). Globally, placer-type gold deposits are also found in the Alder Gulch area, Virginia, Montana. The gold placer is the result of the quartz veins being eroded (Roy et al., 2018). The same thing was also found in the Arizona gold placer deposits associated with schist, granite, and gneiss, where the veins tend to be deeper than the mesothermal and hypothermal types (Youngson T And and Crow, 1999). The gold placer in eastern Siberia is indicated to originate from gold-quartz-low-sulfide types as the primary source due to the mineralogy-geochemical characteristics of the placer

originating from the Lena-Viluy region bordered by rivers (interfluves) (Kazhenkina and Nikiforova, 2016).

Until now there has been no publication of research results related to the type and source of gold mineralization in this area. This study as a preliminary study aims to determine the grain morphology characteristics of mineral composition and metal grade in gold placer deposits in the study area. Based on the regional geological conditions, this area is very promising for the formation of hydrothermal gold mineralization. The Tondong Tallasa area and its surroundings are composed of melange lithology and metamorphic rocks bordering the Propylitized volcanic rocks. Propylite is one of the alteration types/zones

bordering hydrothermal gold mineralization (Hedenquist et al., 2000; Simmons et al., 2005; Sukanto, 1982).

2. Regional Geology

Regionally, Bantimurung area, Tondong Tallasa District, Pangkep Regency is included in the Geological Map Sheet Pangkajene and Watampone Western Part, Sulawesi (Sukanto, 1982). Stratigraphically, the rock formations in and around the study site from oldest to youngest are: Metamorphic Rocks, Melange Complexes, Propylitized Volcanic Rocks, Mallawa Formation, Tonasa Formation, and Diorite Intrusive Rocks (Fig. 2).

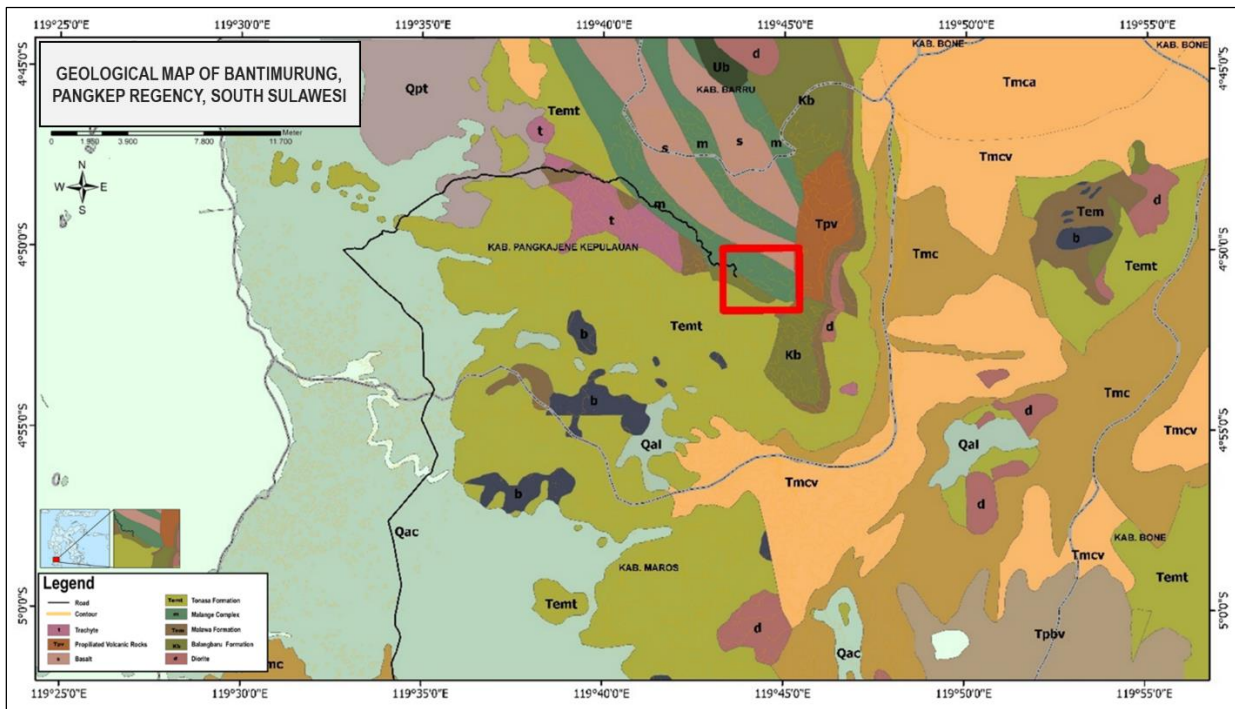


Fig. 2. Regional geological map of the research area and its surroundings. Stratigraphically, the rock formations located at the research site from oldest to youngest are: Metamorphic Rocks, Melange Complexes, Propylitized Volcanic Rocks, Mallawa Formation, Tonasa Formation, and Diorite Intrusive Rocks (Sukanto, 1982)

Metamorphic Rock (s): mostly consisting of schist and few gneiss; contains the minerals glaucophan, garnet, epidote, mica, and chlorite; generally sloping to the northeast, partially brecciated, and reversed to the southwest; this unit is not less than 2000 m thick and has a fault contact with the surrounding rock units; K/Ar dating of schists on east Bantimala yields an age of 111 million years.

Melange Complex (m): tectonic mixed rock consisting of gneiss, breccias, conglomerates, sandstones; gneiss, gray shale, red shale, red radiolarian chert, slate, schist, ultramafic, basalt, diorite and clay; This rock collection is leafy, mostly tilted to the northeast and shears up to the southwest; this unit is not less than 1750 m thick, and has a fault contact with the surrounding rock units; This complex is Mesozoic in age.

Propylitized Volcanic Rocks (Tpv): breccia, lava and tuff; generally andesitic, partially trachytic and basalt; the top is inlaid with red shale and limestone; breccia components vary, from a few cm to more than 50 cm, tuff-bonded which amounts to less than 50%; lava and breccias are dark gray to greenish-grey in color, strongly brecciated and propylitized, containing large amounts of carbonates and silicates; K/Ar dating on basalt east of Bantimala yields an

age of 58.5 million years (Lower Paleocene); this unit is about 400 m thick; unconformably overlain by the Eocene rocks of the Tonasa Formation and the Mallawa Formation; intruded by granodiorite and basalt rocks.

Mallawa Formation (Tem): sandstone, conglomerate, siltstone, claystone, and marl, with inserts of coal and claystone seams or lenses; The sandstones are mostly quartz sandstone, some are arkosic, gneiss, and tuffaceous, generally light gray and light brown in color; generally brittle, less dense; the conglomerate is partially compact; claystone, limestones and marls generally contain unexamined molluscs, and are light gray to dark gray in color; coal in the form of lenses several centimeters thick and in layers up to 1.5 m; based on its fossil content, it is estimated that it is of Eocene age with a parallax to shallow environment; the thickness of this formation is not less than 400 m; overlain with the limestones of the Tonasa Formation and unconformably overlaid by the Propylitized Volcanic Rocks.

Tonasa Formation (Temt): solid coral limestone partially shattered; white and light gray; bioclastic limestone and calcarenite; white light brown and light gray, some well layered, interspersed with tuffaceous globigerina marl; the lower part contains bituminous limestone,

localized with limestone breccia and sandy limestone inserts; near Malawa, in the Camba area, limestone containing glauconite was found, and in several places in the Ralla area limestone was found containing a large amount of schist and ultramafic rock; the layered limestone contains many large foraminifera, the marl contains many small foraminifera and some sandy marl layers contain many large shells (pelecypoda) and snails (gastropods); solid limestones are generally strongly fractured; in the Tanetteriaja area there are three alternating marl lanes with a new layer of limestone; its fossil content indicates an age range from Early Eocene to Middle Miocene, and shallow to deep neritic environments and lagoons; the thickness of this formation is estimated to be not less than 3000 m; superimposed on the rocks of the Malawa Formation and intruded by sills, rifts, and igneous stocks of basalt, trachytic, and diorite composition.

Diorite (d): intrusive of diorite and granodiorite, mainly stock and some cracked, mostly porphyry texture, light gray to gray in color; diorite exposed to the north of Bantimala and to the east of Biru through the sandstone of the Balangbaru Formation and Ultramafic Rocks; the breakthrough that occurred around Camba consisted partly of porphyry granodiorite, with many phenocrysts in the form of biotite and amphibole, and broke through the limestones of the Tonasa Formation and the rocks of the Camba Formation; the dating of K/Ar granodiorite from east of Camba on biotite results in an age of 9.03 million years (Upper Miocene).



Fig. 3. Picturization of sampling station at study area. Boulders of altered Diorite present around sampling station with vein texture indicate mineralization on study area.

Geological structures that develop in this area are reverse and shear faults. reverse fault is a lithological contact between the older Melange Complex and the younger Mallawa Formation. Two shear faults are found in this area, the shear fault in the east has an almost west-east direction and is a lithological contact between the rocks of the Mallawa Formation and the Propylitized Volcanic Rocks. Meanwhile, the shear fault in the west is almost north-south and is a right-hand (dextral) shear fault that shifts the rock blocks of the Tonasa Formation and Mallawa Formation to the south (Fig. 2).

Stream sediment will be found in-side of the river's curve (stations 1, 2, 3, 5, 6, 7, and 8) and between rocks (station 4).

3. Method

3.1 Stream Sediment Sampling

Sampling was carried out using a mini shovel as deep as 30-45 cm in the sediment stream for 350 gram each station (Irfan et al., 2021; Tonggihroh and Nur, 2019). Then the samples were sieved to be separated based on grain size into <10 mesh, 16 mesh, 40 mesh, 70 mesh, and >120 mesh. The sequence of sample numbering is done from

downstream to upstream. Total of 8 stations were sampled along the river towards the upstream with an estimated distance of about 5 km from the placer gold mining location (Fig. 3).

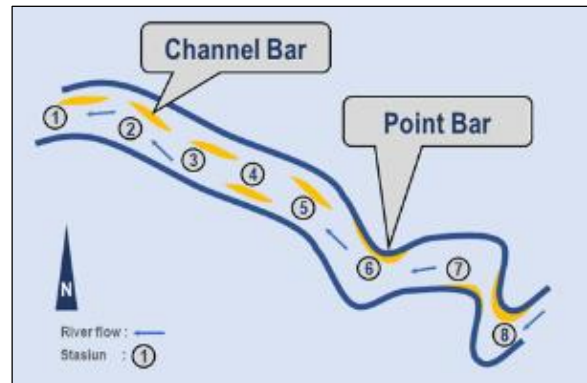


Fig. 4. Types of stream sediment on study area

5 of 8 stations of placer was identified in this study as primary sedimentary bodies occupying the majority of space in this river (channel bar) (Fig. 4) and the rest (station no 6, 7, and 8) was accumulates on the inside bend of streams (point bar) (Hu et al., 2017; Kleinhans and van den Berg, 2011; Olson, 2017).

Table 1. Stations characteristic on study area

Station	Characteristic	
	River flow	Bar
1	Down stream	Channel bar
2	Down stream	Channel bar
3	Down stream	Channel bar
4	Down stream	Channel bar
5	Up stream	Channel bar
6	Up stream	Point bar
7	Up stream	Point bar
8	Up stream	Point bar

3.2 Grain Petrography

Microscopic analysis was carried out by observing the thin section for altered minerals and polishing section for ore minerals using a Nikon Eclipse LV 100N POL polarizing microscope (Husain et al., 2021). Microscopic analysis was also carried out to identify the morphology of the mineral grains. Morphology of grains in this paper refers to grain size, degree of roundness and sphericity of the grains. Microscopic analysis was conducted in the Preparation Room of the Geological Engineering Department, Faculty of Engineering, Hasanuddin University.

3.3 Geochemistry

The grades of Au metal and its associated base metals consisting of Ag, Zn, Pb, and Cu in the placer samples size >120 mesh was analyzed by atomic absorption spectrometry (AAS) method. AAS analysis was carried out using the Buck Scientific Type 205 Atomic Absorption Spectrophotometer at the Analytical Chemistry Laboratory, Department of Chemistry, Faculty of Mathematics and Natural Sciences, Universitas Hasanuddin.

Grade of Au will be compared with other base metal and >120 mesh grain size for correlation analysis.

4. Result

4.1 Grain Size Analysis

Grain size <10 mesh shows random pattern from downstream to upstream, this was caused by the variative size of material on this class of size. Class 16 mesh shows a perfect consistent increasing from downstream to upstream of mass. While class 40 mesh shows random pattern from downstream to upstream, this was caused by the size was between coarse and fine grains. Finally, the class 70 and >120 mesh shows perfect consistent decreasing from downstream to upstream of mass (

). Overall distribution of grain size on study area was towards to sediment transportation theory (Yi et al., 2012).

Based on the graph (Error! Reference source not found.), it can be concluded statistically that the fine grain size, which is <120 mesh from upstream to downstream, has an effect on Ag content for 74.24% (inversely proportional), Cu content for 55.28% (directly

proportional). The concentration of other metals was not significantly affected by grain size, namely Pb 49.74% (inversely proportional), Au 29.05% (directly proportional), Zn 0.63% (inversely proportional).

Table 2. Result of the placer samples grain size measurement

No. ST	Size (Mesh)				
	<10	16	40	70	>120
1	83	20	117	106	24
2	81	24	89	133	24
3	76	72	81	103	18
4	62	84	104	91	10
5	74	86	129	55	6
6	61	103	110	69	7
7	63	111	83	86	6
8	104	135	53	53	4

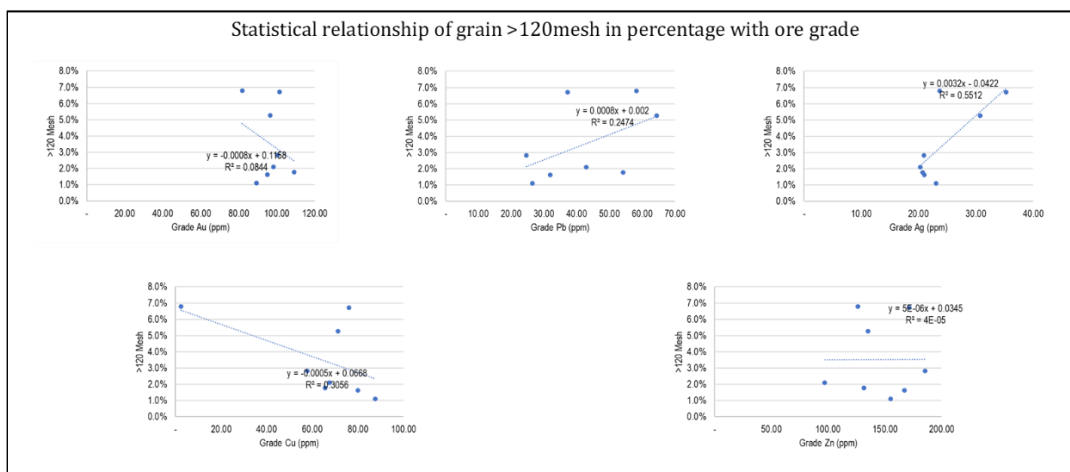


Fig. 5. Statistical relationship of grain >120mesh in percentage with ore grade

4.2 Mineralogy and Grain Morphology

4.2.1 Petrography

The results of microscopic observations showed that 4 minerals were observed (Fig. 6), that is quartz (Qz) with transparent absorption color with white interference color, no pleochroism (-), low intensity, sub-anhedral shape, low relief, no cleavage, conchoidal fragments, mineral size <0.03 mm, has no twins, darkening angle 1-4°.

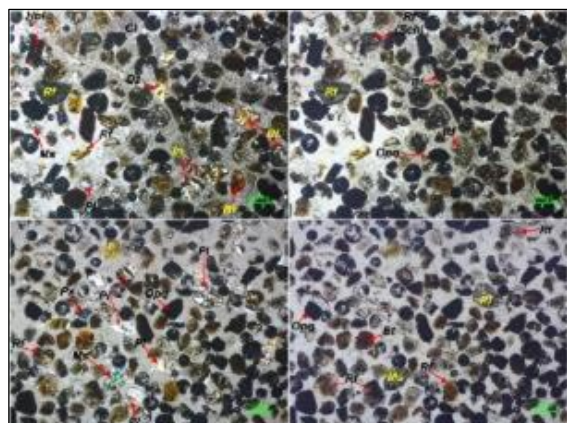


Fig. 6. Photomicrograph of thin-section samples showing mineral features: quartz, plagioclase, biotite, and pyroxenes

Plagioclase abbreviated white gray with gray-black interference color, no pleochroism (-), moderate intensity, sub-anhedral mineral form, moderate relief, one-way perfect mineral cleavage, flat fracture, mineral size 0.05-

0.18 mm, has twins Carlsbad-Albite, dark angle 30-36°, oblique dark type. Pyroxene's absorption color gray with blue-purple-black interference color, high intensity, sub-anhedral shape, high relief, one-way perfect cleavage, flat fragments, mineral size <0.05 mm, no twinning, darkening angle 32-35°, italic dark type. Biotite absorption color is blackish brown with reddish brown interference color, dichroic pleochroism, moderate intensity, sub-anhedral shape, moderate relief, one-way perfect cleavage, flat fracture, mineral size 0.04-0.06 mm, darkening angle 87°.

The results showed that quartz and plagioclase minerals were appear at each station, biotite absence on station 1 and pyroxenes absence on station 2 (Table 3). The abundant of quartz indicate the present of vein, with plagioclase and pyroxene it might be indication of mineralization of epithermal (Burkett et al., 2015; Idrus and Handayani, 2017; Purwanto et al., 2018; Wahyudi, 2011). Biotite present indicate the low sulfidation mineralization (Enríquez et al., 2018; Syafrizal et al., 2017; Villaplaza et al., 2017; Irfan et al., 2017)).

Table 3. Mineral distribution as a result of microscopic observations on thin-section samples to the distribution of stations

No	Mineral	Station							
		1	2	3	4	5	6	7	8
1	Quartz	✓	✓	✓	✓	✓	✓	✓	✓
2	Plagioclase	✓	✓	✓	✓	✓	✓	✓	✓
3	Biotite	-	✓	✓	✓	✓	✓	✓	✓
4	Pyroxenes	✓	✓	-	✓	✓	✓	✓	✓

The grain morphology of the thin section observation (Fig. 7) shows that quartz has a high sphericity at stations 1, 2, 3, 5, 6, and 8. While at stations 4 and 7 it has a low sphericity. The character of roundness tends to be very angular to sub-rounded from upstream to downstream of the river. Plagioclase tends to have sub rounded roundness

and high sphericity at all stations. Biotite tends to have a high sphericity with roundness from upstream to downstream is very angular, then angular, then sub-rounded. Pyroxenes tend to have high sphericity with very angular and angular roundness.

Mineral	Station							
	1	2	3	4	5	6	7	8
Quartz								
Roundness	Sub-rounded	Very angular	Very angular	Sub-rounded	Sub-rounded	Angular	Very angular	Very angular
Sphericity	High	High	High	low	High	High	low	High
Plagioclase								
Roundness	Sub-rounded	Sub-rounded	Sub-rounded	Sub-rounded	Sub-rounded	Sub-rounded	Sub-rounded	Sub-rounded
Sphericity	High	High	High	High	High	High	High	High
Biotite	Absence							
Roundness		Sub-rounded	Sub-rounded	Angular	Very angular	Angular	Very angular	Sub-rounded
Sphericity		High	High	High	High	low	High	High
Pyroxenes			Absence					
Roundness	low	Very angular		Angular	Angular	Angular	Angular	Very angular
Sphericity		High		High	High	low	High	low

Fig. 7. Morphology characteristics (roundness and sphericity) of alteration mineral grain.

4.2.2 Ore petrography

The results of microscopic observations (Fig. 8) showed 10 ore mineral were observed (Table 4) namely cassiterite (cst) with blackish gray color, anhedral shape, anisotropic, no pleochroism, mineral size 0.1-0.5 mm found at stations 1, 4, 5, and 7. Silver (ag) is bright white, subhedral-anhedral form, isotropic, no pleochroism, mineral size <0.3 mm found at stations 1, 3, 4, 6, 7, and 8.

Table 4 Mineral distribution as a result of microscopic observations on thin-section samples to the distribution of stations

No	Mineral	Station							
		1	2	3	4	5	6	7	8
1	Cassiterite	✓			✓	✓		✓	
2	Silver	✓		✓	✓		✓	✓	✓
3	Chalcopyrite	✓	✓		✓	✓			✓
4	Pyrite	✓	✓	✓	✓	✓		✓	✓
5	Covellite	✓							✓
6	Magnetite		✓						
7	Sphalerite			✓				✓	
8	Garnet			✓					
9	Tennantite					✓	✓	✓	
10	Gold								✓

Chalcopyrite (cp) is bright yellow in color, anhedral form, anisotropic, no pleochroism, mineral size of 0.05 mm is found at stations 1, 2, 4, 5, and 8. Pyrite (py) is yellowish white, subhedral-anhedral form, there is striation, anisotropic, does not have pleochroism, mineral size 0.1 - 0.3 mm is found at all stations except station 6.

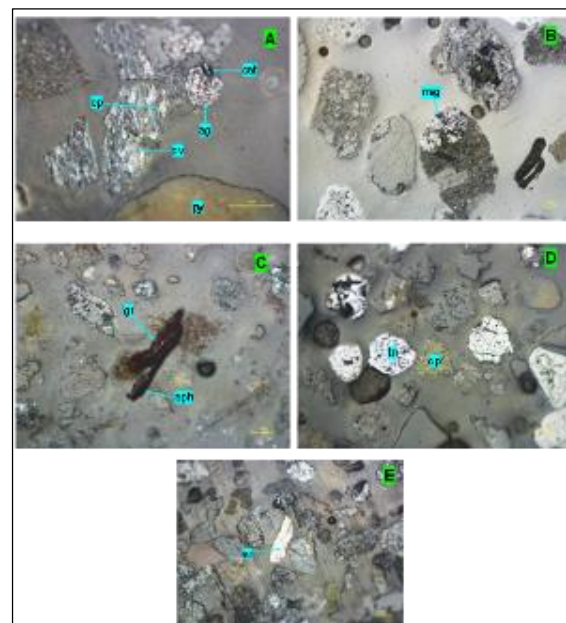


Fig. 8. Photomicrograph of a polished incision sample showing: cassiterite, silver, chalcopyrite, pyrite, dan covellite (A); magnetite (B); sphalerite dan garnet (C); chalcopyrite dan tennantite (D); dan gold (E)

Covellite (cv) Blue color, anhedral shape, does not have pleochroism, mineral size 0.005 mm is found at station only found at stations 1 and 8. Magnetite (mag) Blackish gray color, euhedral-subhedral form, isotropic, no pleochroism, mineral size <0.25 mm found only at station 2. Sphalerite (sph) Gray color, shape subhedral-anhedral, isotropic, no pleochroism, mineral size 125 m found at stations 3 and 7.

Garnet (gr) Brown color, anhedral shape, anisotropic, no pleochroism, mineral size 0.3 mm found at station 3. Tennantite (tn) Grayish white color, sub shape hedral-anhedral, anisotropic, no pleochroism, size <0.025 mm found at stations 5, 6, and 7. Gold (au) Golden yellow, euhedral form, isotropic, lacks pleochroism, mineral crystal size 0.1-0.3 cm was found at station 8. Mineragraphic observations showed pyrite was present at almost every station. Next is silver also found quite a lot along the station. Meanwhile, covellite, magnetite, sphalerite, and garnet were found only slightly at the sampling station.

Grain morphology Observations of polished section (Fig. 9) showed Cassiterite has a low sphericity. The roundness character is sub-roundness at station 1 then decreases to very angular at stations 4 and 5, and becomes angular at station 7. Sliver has a high sphericity where the roundness character tends to be sub-rounded at stations 1, 3, 7, and 8, and becomes angular at stations 6 and 8. Chalcopyrite has a high sphericity at stations 4, 5, and 8 while at stations 1 and 2 it has a low sphericity. The roundness character from upstream to downstream is very angular then angular and becomes sub-rounded. Pyrite has a high sphericity. The roundness character of pyrite is sub-angular at station 1, then becomes very angular at stations 4, 5 and 7, and becomes angular at stations 7 and 8. Covellite has a high sphericity where roundness from upstream to downstream

is angular and then becomes sub-rounded. Magnetite has a low sphericity with very angular roundness. Sphalerite has a low sphericity with very angular roundness. Garnet has a low sphericity with very angular roundness. Tennantite has a high sphericity with sub-angular roundness. Gold has a low sphericity with very angular roundness.

High sulfidation epithermal deposits are characterized by the assemblage of enargite - luzonite - covellite and pyrite sulfide ore minerals, low sulfidation epithermal by pyrite - pyrrhotite - arsenopyrite and Fe-rich sphalerite, and intermediate sulfidation epithermal by tennantite - tetrahedrite - low-Fe- chalcopyrite and sphalerite (Einaudi et al., 2003; Sillitoe and Hedenquist, 2003; Simmons et al., 2005).

Ore petrographic (mineragraphic) observations show that pyrite is present at almost every station. Next is silver is also found quite a lot along the station. Meanwhile, covellite, magnetite, sphalerite, and garnet were found only slightly at the sampling station. This mineral composition indicates that the source of the placer deposits at the study site is epithermal low sulfidation or epithermal high sulfidation (Aluç et al., 2020; Burkett et al., 2015; Enríquez et al., 2018; Idrus and Handayani, 2017; Pratomo et al., 2021; Purwanto et al., 2018; Syafrizal et al., 2017; Villaplaza et al., 2017; Wahyudi, 2011).

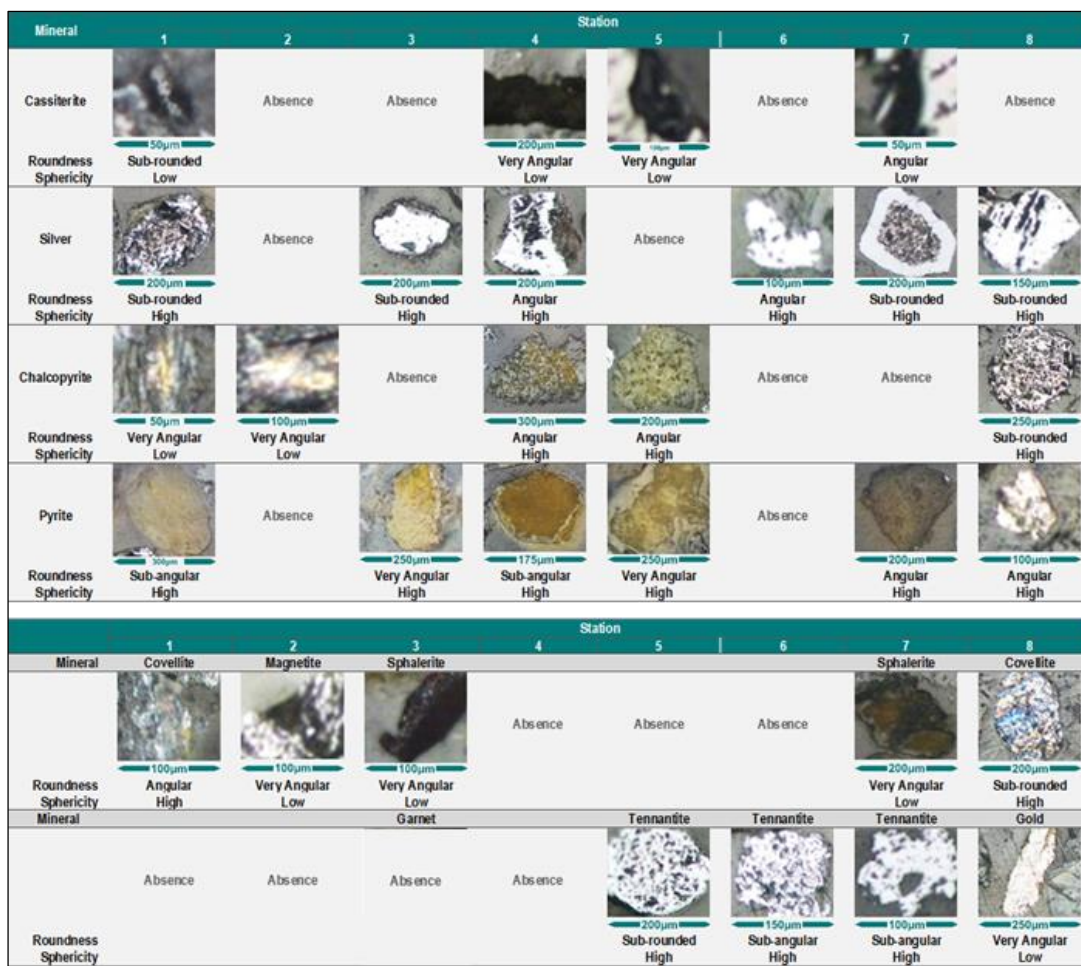


Fig. 9. Morphology characteristics (roundness and sphericity) of ore mineral grain

4.3 Grade of Au and Its Associated Metals

The results showed that the distribution of the value of Au varied along the river. Au content is directly

proportional to Cu and inversely proportional to Zn, Pb, and Ag. Statistically Au affects the content of Cu by 50.97%. However statistically station 1 shows only 2,5 ppm of Cu

compares to other station it could reach to 72,3 ppm in average.

Table 5. The results of AAS analysis of the grade of Ag, Au, Cu, Pb, and Zn metals from the placer samples in the research area

ST	Grade (ppm)				
	Au	Cu	Pb	Zn	Ag
1	81,8	2,5	58,2	126,4	23,7
2	101,4	76,1	37,3	171,7	35,3
3	96,5	71,3	64,5	135,0	30,7
4	100,5	57,8	24,7	185,5	21,0
5	109,1	65,6	54,3	131,5	20,7
6	98,2	67,6	43,0	97,1	20,3
7	95,0	80,1	31,9	167,1	21,0
8	89,3	87,7	26,5	155,0	23,1

Based on the results of statistical analysis of geochemical data as described above, it can be concluded that Au is genetically associated with Cu, and vice versa not associated with minerals carrying the elements Zn, Pb, and Ag because it has a negative correlation with Au, this may be because the source placer is an Au-Cu deposit.

Table 6. Relation of gold to associated metal at the study area.

No	Element	Relation with Au	R2(%)	r
1	Cu	Direction	25.98	50.97%
2	Zn	Inverse	1.52	12.33%
3	Pb	Inverse	0.3	5.47%
4	Ag	Inverse	1.52	12.33%

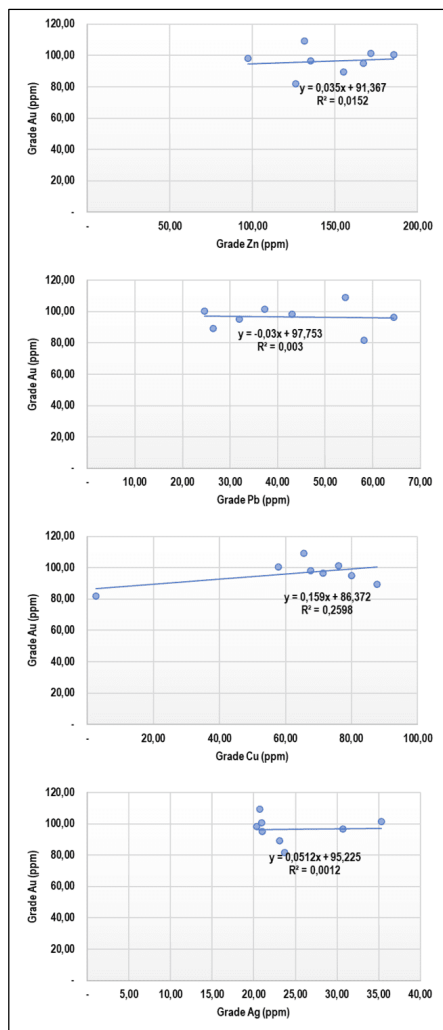


Fig. 10. Statistical relationship of grain Au with other base metal (Zn, Pb, Cu, and Ag) on study area

Au grade correlated with stream sediment types it is 97,86 ppm for channel bar and 94,16 ppm for point bar, based on this we conclude the downstream has higher grade of Au compare to the upstream.

Microscopic observations show Au was appear at station 8 only, but on AAS Au was found along the station, this could be caused by Au grains that were still attached into the mineral carrier and had not been separated from other minerals so that it could not be seen visually. This can also indicate that the source of this placer deposit is not far from the study site.

5. Discussion

The percentage of grain size >120, 70, and 40 mesh tends to increase from upstream to downstream of the river, and vice versa for grain-sized 16 and <10 mesh. The grain morphology of the thin-section observation shows that quartz dominant has high sphericity with the character of roundness that tends to be very angular to sub-rounded from upstream to downstream of the river. Plagioclase tends to have sub-rounded roundness and high sphericity. Muscovite has low sphericity at stations upstream, then becomes high downstream. The roundness of muscovite from upstream to downstream is very angular, angular, and then sub-rounded. Hornblende tends to have low sphericity with roundness from upstream to downstream is very angular, then angular, then sub-rounded. Biotite tends to have high sphericity with roundness from upstream to downstream is very angular, then angular, then sub-rounded. Pyroxenes tend to have high sphericity with very angular and angular roundness. Grain morphology shows the presence of angular and very angular roundness, a variety of sphericity from high to low even the presence of altered diorite boulder with quartz vein it is clear the source of the anomaly of base metal in the study area is quite near. It has a strong indication the source might be from the diorite intrusion in the east of the study area.

Au grade is 97,86 ppm for channel bar and 94,16 ppm for point bar, and the distribution of Au grades increases in the river from upstream to downstream, and the range of Au grades is 81.79 - 109.14 ppm with an average of 96.47 ppm. Based on this we conclude the downstream has a higher grade of Au compared to the upstream. The average grade of Cu at the study site was 63.5775 ppm with a range of 2.5 - 87.66 ppm, the grade of Cu constantly increased from stations 4 to 8. The average grade of Ag was 24,475 ppm with a range of 20.3 - 35,3 ppm, Ag grade tends to increase from upstream to downstream at station 2. The average grade of Pb is 42.5325 ppm with a range of 24.68 - 64.46 ppm, Pb grade increase from station 8 to station 5 then Pb grade becomes varied from station 4 to station 1. The average grade of Zn was 146.15 with a range of 97.06 - 185.52 ppm Zn grade distribution did not show a significant pattern. The results showed that the distribution of the value of the element Au content varied along the river. Au content is directly proportional to Cu content and inversely proportional to Zn, Pb, and Ag. Statistically, Au affects the content of Cu by 50.97%.

The grain morphology of the thin-section observation shows that quartz dominant has high sphericity with a character of roundness that tends to be very angular to sub-rounded from upstream to downstream of the river. Plagioclase tends to have sub-rounded roundness and high sphericity. Muscovite has low sphericity at stations upstream, then becomes high downstream. The roundness of muscovite from upstream to downstream is very angular, angular, and then sub-rounded. Hornblende tends to have

low sphericity with roundness from upstream to downstream is very angular, then angular, then sub-rounded. Biotite tends to have high sphericity with roundness from upstream to downstream is very angular, then angular, then sub-rounded. Pyroxenes tend to have high sphericity with very angular and angular roundness.

In microscopic observations, Au metal was found at station 8 only, but on AAS Au was found along with the station, this could be caused by Au grains that were still attached to the mineral and had not been separated from other minerals so that it could not be seen visually. This can also indicate that the source of this placer deposit is not far from the study site. Au-grain during transporting from upstream after being released from associated minerals will stick to other Au-grain all the way downstream, this might cause the small percentage of Au on fine grain.

Petrography shows abundant quartz indicates the presence of veins; it might be an indication of mineralization of epithermal (Irfan et al., 2017); (Nur et al., 2019). Ore petrography shows pyrite present along the river, silver is also found quite a lot along the river. Meanwhile, covellite, magnetite, sphalerite, and garnet were found only slightly at the sampling station. This mineral composition indicates that the source of the placer deposits at the study site is epithermal low sulfidation or epithermal high sulfidation (Aluç et al., 2020; Burkett et al., 2015; Enríquez et al., 2018; Idrus and Handayani, 2017; Pratomo et al., 2021; Purwanto et al., 2018; Syafrizal et al., 2017; Villaplaza et al., 2017; Wahyudi, 2011). Although Au-grain visually on microscope present only on 1 station it could be cause the location is quite near of mineralization so the Au-grain is still in very fine grain size which it's hard to identify through microscope beside that the Au-grain might be still trapped in carrier mineral is the other reason Au-grain doesn't appear on ore petrography but appear on chemistry analysis.

Geochemistry shows that the distribution of Au varied along the river. Au content is directly proportional to Cu and inversely proportional to Zn, Pb, and Ag. Statistically Au affects the content of Cu by 50.97%. However statistically station 1 shows only 2,5 ppm of Cu compares to other station it could reach to 72,3 ppm in average. It can be concluded that Au is genetically associated with Cu, and vice versa not associated with minerals carrying the elements Zn, Pb, and Ag because it has a negative correlation with Au, this may cause the source placer is an Au-Cu deposit or epithermal high sulfidation.

6. Conclusion

- Metallic minerals identified from the study site are cassiterite, covellite, magnetite, sphalerite, garnet, tennantite, and gold as well as abundant silver, chalcopyrite, and pyrite, while the transparent minerals identified are quartz, plagioclase, muscovite, hornblende, clay minerals, biotite, and pyroxenes.
- Morphologically mineral transparent was very angular until sub-rounded, as well metallic minerals except gold and sphalerite was very angular caused of source relative closer which is diorite intrusion on the east of study area.
- Au is genetically associated with Cu; this may cause the Au grade statistically was correlated with Cu grade and also the ore petrography.
- The range of Au grades at the study site was 81.79 - 109.14 ppm with an average of 96.47 ppm, that the distribution of relative grade increases in the river from upstream to downstream as well as grades of Cu

statistically directly proportional from upstream to downstream.

Acknowledgements

This research has been financially supported by Penelitian Tesis Magister from the Directorate of Research and Community Service, Directorate General of Research and Development Strengthening Ministry of Research, Technology, and Higher Education of the Republic of Indonesia. We would like to acknowledge the Geochemical and mineral laboratory, Geological Department, and Analytical Chemistry Laboratory, Universitas Hasanuddin for ore petrography and metal analysis preparation.

References

- Aluç, A., Kuşcu, İ., Peytcheva, I., Cihan, M., von Quadt, A., 2020. The late Miocene Öksüt high sulfidation epithermal Au-Cu deposit, Central Anatolia, Turkey: Geology, geochronology, and geochemistry. *Ore Geology Reviews* 126. <https://doi.org/10.1016/j.oregeorev.2020.103795>
- Burkett, D., Graham, I., Spencer, L., Lennox, P., Cohen, D., Zwingmann, H., Lau, F., Kelly, B., Cendón, D., 2015. The Kulumadau epithermal breccia-hosted gold deposit, Woodlark Island, Papua New Guinea. *PACRIM Australasian Institute of Mining and Metallurgy (The AusIMM)* 1-8.
- Carlile, J.C., Digdowirogo, S., Darius, K., 1990. Geological setting, characteristics and regional exploration for gold in the volcanic arcs of North Sulawesi, Indonesia. *Journal of Geochemical Exploration* 35, 105-140.
- Carlile, J.C., Mitchell, A.H.G., 1994. Magmatic arcs and associated gold and copper mineralization in Indonesia. *Journal of Geochemical Exploration* 50, 91-142.
- Darman, H., Sidi, F.H., 2000. An outline of the geology of Indonesia Play Fairways in SE Asian Basins View project. *Indonesian Association of Geologists (IAGI)* 192.
- Einaudi, M.T., Hedenquist, J.W., Esra Inan, E., 2003. Sulfidation state of fluids in active and extinct hydrothermal systems: transitions from porphyry to epithermal environments. *Society of Economic Geologists Special Publication* 285-313.
- Enríquez, E., Iriondo, A., Camprubí, A., 2018. Geochronology of Mexican mineral deposits. VI: The Tayoltita lowsulfidation epithermal Ag-Au district, Durango and Sinaloa. *Boletín de la Sociedad Geológica Mexicana* 70, 531-547. <https://doi.org/10.18268/BSGM2018v70n2a13>
- Hall, R., Wilson, M.E.J., 2000. Neogene sutures in eastern Indonesia. *Journal of Asian Earth Sciences* 18, 781-808.
- Hedenquist, J., Arribas, A., Gonzalez-Urien, E., 2000. Exploration for epithermal gold deposits porphyry copper genesis and exploration view project The Giant Grasberg porphyry system View project. *Reviews in Economic Geology* 13, 245-277.
- Hu, G.M., Ding, R.X., Li, Y.B., Shan, J.F., Yu, X.T., Feng, W., 2017. Role of flood discharge in shaping stream geometry: Analysis of a small modern stream in the Uinta Basin, USA. *Journal of Palaeogeography* 6, 84-95. <https://doi.org/10.1016/j.jop.2016.10.001>
- Husain, A.A., Nur, I., Sufriadin, Irfan, U.R., 2021. Recommendation for lateritic Ni-ore processing: Garnierite mineralogical and geochemical approach, in: *IOP Conference Series: Earth and Environmental*

- Science. IOP Publishing Ltd. <https://doi.org/10.1088/1755-1315/921/1/012029>
- Idrus, A., Handayani, E., 2017. Geology and Characteristic of Low Sulphidation Epithermal Vein in Senepo Area, East Java. *INDONESIAN MINING JOURNAL* 20, 93–103.
- Idrus, A., Nur, I., 2011. Hydrothermal ore mineralization in Sulawesi: a view point of tectonic setting and metallogenesis. *Proceedings of the Joint Convention HAGI-IAGI* 26–29.
- Idrus, A., Prihatmoko, S., Harjanto, E., Meyer, F.M., Nur, I., Widodo, W., Agung, L.N., 2017. Metamorphic rock-hosted orogenic gold deposit style at Bombana (Southeast Sulawesi) and Buru Island (Maluku): Their key features and significances for gold exploration in Eastern Indonesia. *Journal of Geoscience, Engineering, Environment, and Technology* 2, 124. <https://doi.org/10.24273/jgeet.2017.2.2.291>
- Irfan, U.R., Nur, I., Kasim, M., 2017. Hydrothermal alteration mineralogy associated with gold mineralization in Buladu Area, Gorontalo, Northern Sulawesi, Indonesia. *Int. J. Adv. Sci. Eng. Inf. Technol.* 7, 2244–2250. <https://doi.org/10.18517/ijaseit.7.6.3837>
- Irfan, U.R., Maulana, A., Nur, I., Thamrin, M., Manaf, M., 2021. Evaluation of heavy metal (Cu, Pb, Zn) distribution in base metal mining area at Sangkaropi: Implication for land use planning. in: *IOP Conference Series: Earth and Environmental Science*. IOP Publishing Ltd. <https://doi.org/10.1088/1755-1315/921/1/012047>
- Kavaleris, I., Leeuwen, T.M. van, Wilson, M., Kalosi, P.T., 1992. Geological setting and styles of mineralization, north arm of Sulawesi, Indonesia, *Journal of Southeast Asian Earth Sciences*.
- Kazhenkina, A.G., Nikiforova, Z.S., 2016. Types of Primary Sources of Placer Gold of the East Siberian Platform (Lena-Viluy Interfluve), in: *IOP Conference Series: Earth and Environmental Science*. Institute of Physics Publishing. <https://doi.org/10.1088/1755-1315/44/4/042013>
- Kleinhans, M.G., van den Berg, J.H., 2011. River channel and bar patterns explained and predicted by an empirical and a physics-based method. *Earth Surface Processes and Landforms* 36, 721–738. <https://doi.org/10.1002/esp.2090>
- Nur, I., Idrus, A., Pramumijoyo, S., Harijoko, A., Imai, A., 2011. Mineral paragenesis and fluid inclusions of the Bincai epithermal silver-base metal vein at Baturappe area, South Sulawesi, Indonesia. *Journal of Applied Geology* 3. <https://doi.org/10.22146/jag.7179>
- Nur, I., Sufriadin, Ilyas, A., Irfan, U.R., 2019. Hydrothermal Alteration Associated with Vein-Type Sulphide Mineralization at Lappadata Prospect, South Sulawesi, Indonesia: A Preliminary Study. *IOP Conf. Ser. Mater. Sci. Eng.* 676. <https://doi.org/10.1088/1757-899X/676/1/012033>
- Olson, L.M., 2017. Channel Bar Morphology, Distribution, And Mining-Related Geochemistry In The Big River, St. Francois County, Missouri: Implications For Geomorphic Recovery. *BearWorks*, the institutional repository of Missouri State University. 1–157.
- Pratomo, S.U., Titisari, A.D., Idrus, A., 2021. Hydrothermal Alteration of High Sulphidation Epithermal Deposits in Secang Area, Tulungagung, East Java, Indonesia. *Journal of Applied Geology* 5, 73. <https://doi.org/10.22146/jag.55235>
- Purwanto, H.S., Suharsono, Puntadewa, A., 2018. Epithermal Cu-Pb-Zn mineralization in the Cidolog Area, Sukabumi Regency West Java Province, Indonesia, in: *IOP Conference Series: Earth and Environmental Science*. Institute of Physics Publishing. <https://doi.org/10.1088/1755-1315/212/1/012028>
- Roy, S., Upton, P., Craw, D., 2018. Gold in the hills: patterns of placer gold accumulation under dynamic tectonic and climatic conditions. *Mineralium Deposita* 53, 981–995. <https://doi.org/10.1007/s00126-017-0789-6>
- Sillitoe, R., Hedenquist, J., 2003. Linkages between volcanotectonic settings, ore-fluid compositions, and epithermal precious-metal deposits. *Society of Economic Geologists* 315–343.
- Simmons, S.F., White, N.C., John, D.A., 2005. Geological Characteristics of Epithermal Precious and Base Metal Deposits. *Economic Geology* 100th Anniversary 485–522.
- Sukanto, R., 1982. Geologic map of the Pangkajene and western part of Watampone quadrangles Sulawesi. Geological Research and Development Centre.
- Syafrizal, Rivai, T.A., Yonezu, K., Kusumanto, D., Watanabe, K., Hede, A.N.H., 2017. Characteristics of a low-sulphidation epithermal deposit in the River Reef Zone and the Watuputih Hill, the Poboya gold prospect, Central Sulawesi, Indonesia: Host rocks and hydrothermal alteration. *Minerals* 7. <https://doi.org/10.3390/min7070124>
- Tonggiroh, A., Nur, I., 2019. Geochemical correlation of gold placer and indication of Au-Cu-Pb-Zn-Ag mineralization at Parigi Moutong, Central Sulawesi, Indonesia, in: *Journal of Physics: Conference Series*. Institute of Physics Publishing. <https://doi.org/10.1088/1742-6596/1341/5/052003>
- van Leeuwen, T., 2018. Twenty Five More Years of Mineral Exploration and Discovery in Indonesia (1993-2017). *Masyarakat Geologi Ekonomi Indonesia* 1, 1–37.
- van Leeuwen, T., Pieters, P.E., 2011. Mineral deposits of Sulawesi. *Proceedings of The Sulawesi Mineral Resources 2011 Seminar MGEI-IAGI* 1–130. <https://doi.org/10.13140/2.1.3843.2322>
- Villaplaza, B.R.B., Buena, A.E., Pacle, N.A.D., Payot, B.D., Gabo-Ratio, J.A.S., Ramos, N.T., Dimalanta, C.B., Faustino-Eslava, D. v., Queaño, K.L., Yumul, G.P., Yonezu, K., 2017. Alteration and lithogeochemistry in the Masara gold District, Eastern Mindanao, Philippines, as tools for exploration targeting. *Ore Geology Reviews* 91, 530–540. <https://doi.org/10.1016/j.oregeorev.2017.09.004>
- Wahyudi, T., 2011. Mineralogical Characters of Karang Paningal Epithermal Vein Deposits, West Java. *Indonesian Mining Journal* 14, 54–62.
- Yi, L., Yu, H., Ortiz, J.D., Xu, X., Qiang, X., Huang, H., Shi, X., Deng, C., 2012. A reconstruction of late Pleistocene relative sea level in the south Bohai Sea, China, based on sediment grain-size analysis. *Sedimentary Geology* 281, 88–100. <https://doi.org/10.1016/j.sedgeo.2012.08.007>
- Youngson T And, J.H., Craw, D., 1999. Variation in Placer Style, Gold Morphology, and Gold Particle Behavior Down Gravel Bed-Load Rivers: An Example from the

Shotover/Arrow-Kawarau-Clutha River System,
Otago, New Zealand, Economic Geology.



© 2022 Journal of Geoscience, Engineering,
Environment and Technology. All rights reserved.
This is an open access article distributed under the
terms of the CC BY-SA License (<http://creativecommons.org/licenses/by-sa/4.0/>).
